

# Hsp70 stabilizes lysosomes and reverts Niemann–Pick disease-associated lysosomal pathology

Thomas Kirkegaard<sup>1</sup>, Anke G. Roth<sup>2</sup>, Nikolaj H. T. Petersen<sup>1</sup>, Ajay K. Mahalka<sup>3</sup>, Ole Dines Olsen<sup>1,4</sup>, Irina Moilanen<sup>3</sup>, Alicja Zylicz<sup>5</sup>, Jens Knudsen<sup>4</sup>, Konrad Sandhoff<sup>6</sup>, Christoph Arenz<sup>2</sup>, Paavo K. J. Kinnunen<sup>3</sup>, Jesper Nylandsted<sup>1</sup> & Marja Jäättelä<sup>1</sup>

Heat shock protein 70 (Hsp70) is an evolutionarily highly conserved molecular chaperone that promotes the survival of stressed cells by inhibiting lysosomal membrane permeabilization<sup>1–5</sup>, a hallmark of stress-induced cell death<sup>6–10</sup>. Clues to its molecular mechanism of action may lay in the recently reported stress- and cancer-associated translocation of a small portion of Hsp70 to the lysosomal compartment<sup>11</sup>. Here we show that Hsp70 stabilizes lysosomes by binding to an endolysosomal anionic phospholipid bis(monoacylglycerol)phosphate (BMP), an essential co-factor for lysosomal sphingomyelin metabolism<sup>12–14</sup>. In acidic environments Hsp70 binds with high affinity and specificity to BMP, thereby facilitating the BMP binding and activity of acid sphingomyelinase (ASM). The inhibition of the Hsp70–BMP interaction by BMP antibodies or a point mutation in Hsp70 (Trp90Phe), as well as the pharmacological and genetic inhibition of ASM, effectively revert the Hsp70-mediated stabilization of lysosomes. Notably, the reduced ASM activity in cells from patients with Niemann–Pick disease (NPD) A and B—severe lysosomal storage disorders caused by mutations in the sphingomyelin phosphodiesterase 1 gene (*SMPD1*) encoding for ASM<sup>15</sup>—is also associated with a marked decrease in lysosomal stability, and this phenotype can be effectively corrected by treatment with recombinant Hsp70. Taken together, these data open exciting possibilities for the development of new treatments for lysosomal storage disorders and cancer with compounds that enter the lysosomal lumen by the endocytic delivery pathway.

To test whether the lysosomal localization is crucial for the reported ability of Hsp70 to stabilize lysosomal membranes<sup>1</sup>, we took advantage of the endocytic machinery of cells to target recombinant Hsp70 (rHsp70) into the lysosomes. Immunocytochemical and biochemical analysis of U-2-OS osteosarcoma cells incubated with fluorochrome-labelled rHsp70 (rHsp70-AF488) showed effective uptake of rHsp70, its specific co-localization with late endosomal and lysosomal markers, and binding to lysosomal membranes (Fig. 1a, b and Supplementary Fig. 1). Using real-time imaging to monitor lysosomal membrane integrity (Fig. 1c and Supplementary Movie 1), we showed that the endocytosed rHsp70 protected lysosomes against photo-oxidation (Fig. 1d). Furthermore, short interfering RNA (siRNA)-mediated depletion of Hsp70 sensitized the lysosomes to photo-oxidation, and this effect was fully reverted by endocytosed rHsp70, aptly demonstrating that the protective effect of endogenous Hsp70 is mediated by the small fraction of the protein in the lysosomal lumen (Fig. 1e). In spite

of similar uptake (data not shown), no lysosomal stabilization was observed with recombinant Hsc70 and Hsp70-2, which share 86% and 84% amino acid sequence homology with Hsp70 (ref. 16), respectively (Fig. 1d).

The presence of Hsp70 in the lysosomal membranes and its ability to survive the hydrolytic lysosomal environment suggest that it binds to the lysosomal membrane lipids. Thus, we investigated the interaction of Hsp70 with palmitoyl-oleoyl-phosphatidylcholine (POPC) large unilamellar vesicles (LUVs) containing various anionic lipids, that is, palmitoyl-oleoyl-phosphatidylserine (POPS; primarily in plasma membrane), cardiolipin (primarily mitochondrial) and BMP (primarily in late endosomes/lysosomes). Taking into account the increasingly acidic milieu of the endolysosomal compartment after maturation to lysosomes, we compared the protein–lipid interactions in neutral (pH 7.4) and acidic (pH 4.5) conditions (Fig. 2a). At pH 7.4, rHsp70 caused a small relative change in the 90° light scattering in the tested liposomes, indicating weak binding. Notably, lowering the pH to 4.5 greatly enhanced the binding to all negatively charged lipids, and especially to BMP, whereas the binding to POPC was not significantly increased after acidification (Fig. 2a). The high affinity binding of Hsp70 to BMP in acidic pH was confirmed in an independent set of BIAcore experiments (Fig. 2d). Notably, BMP antibodies delivered to the endolysosomal compartment by endocytosis<sup>17</sup> effectively inhibited the ability of rHsp70 to stabilize the lysosomes in living cells, suggesting that Hsp70–BMP binding is essential for the pro-survival function of Hsp70 (Fig. 2b).

To investigate which part of the Hsp70 protein is responsible for the BMP binding, we measured the fluorescence shift of tryptophan residues after the docking of rHsp70 and its mutants into BMP-containing liposomes. The loss of signal in relative peak fluorescence intensity for the Hsp70 mutant lacking amino acids 119–426 in the amino-terminal ATPase domain (rHsp70- $\Delta$ ATP), but not for that lacking amino acids 437–617 in the carboxy-terminal peptide-binding domain (rHsp70- $\Delta$ PBD), indicated that the ATPase domain was required for the high-affinity binding of Hsp70 to BMP (Fig. 2c). Next, we substituted the two tryptophan residues in Hsp70 with phenylalanine (Trp90Phe and Trp580Phe) and studied which tryptophan is responsible for the fluorescence shift induced by lipid binding. The reduction of the signal with rHsp70(Trp90Phe) only indicated that the N terminus of the protein docked into the lipid layer (Fig. 2c). A more quantitative BIAcore analysis of the BMP–rHsp70 interaction confirmed that Hsp70 interacted with BMP

<sup>1</sup>Apoptosis Department and Centre for Genotoxic Stress Research, Institute of Cancer Biology, Danish Cancer Society, DK-2100 Copenhagen, Denmark. <sup>2</sup>Institute for Chemistry, Humboldt University, D-10099 Berlin, Germany. <sup>3</sup>Helsinki Biophysics & Biomembrane Group, Institute of Biomedicine, University of Helsinki, FIN-00014 Helsinki, Finland. <sup>4</sup>Department of Biochemistry and Molecular Biology, University of Southern Denmark, DK-5230 Odense, Denmark. <sup>5</sup>International Institute of Molecular and Cell Biology, 02-109 Warsaw, Poland. <sup>6</sup>LIMES c/o Kekulé-Institute for Organic Chemistry and Biochemistry, University of Bonn, D-53121 Bonn, Germany.

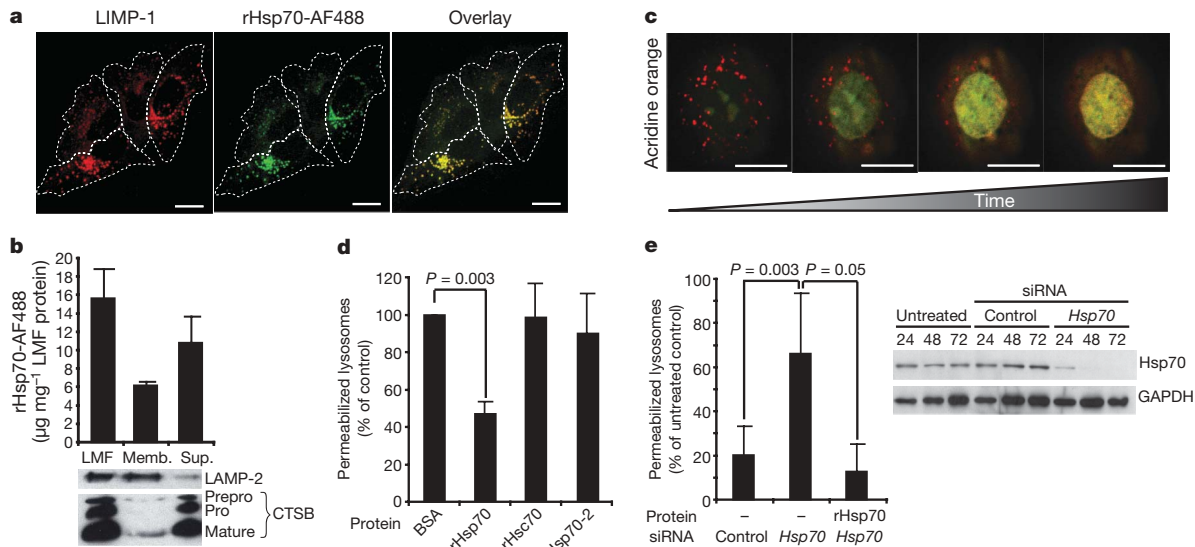


**Figure 1 | Lysosomal Hsp70 stabilizes lysosomal membranes.**

**a**, Representative confocal images of U-2-OS cells incubated with 300 nM rHsp70-AF488 (green) for 24 h, fixed and stained for lysosomal integral membrane protein-1 (LIMP-1, also known as CD63; red). Dotted lines illustrate cell borders. Co-localization coefficients for rHsp70-AF488 and LIMP-1 were  $0.935 \pm 0.54$  (Pearson's) and  $1.00 \pm 0.00$  (Mander's). For co-localization with other organelle markers see Supplementary Fig. 1. **b**, U-2-OS cells were incubated with 300 nM rHsp70-AF488 for 24 h before quantification of rHsp70-AF488 in membranes (memb.) and supernatant (sup.), obtained by repeated freeze/thaw cycles and centrifugation of the light membrane fraction (LMF). The immunoblot analyses of lysosome-associated membrane protein 2 (LAMP-2) and cathepsin B (CTSB) demonstrate the validity of the fractionation procedure. **c**, Representative

still images of U-2-OS cells exposed to photo-oxidation (acridine orange and blue light). The loss of lysosomal integrity is visualized by the loss of red and increase in green staining (see Supplementary Movie 1 for the whole sequence). Scale bars (**a** and **c**), 20  $\mu\text{m}$ . **d**, **e**, U-2-OS cells were incubated with 300 nM bovine serum albumin (BSA; negative control) or indicated recombinant proteins for 24 h, and analysed for lysosomal integrity after photo-oxidation. When indicated, cells were treated with siRNAs for 48 h before the addition of recombinant proteins (**e**). Representative immunoblots of indicated proteins from U-2-OS cells left untreated or treated with control or *Hsp70* siRNAs are shown on the right. All values represent means  $\pm$  s.d. for minimum of three independent experiments.

mainly through its ATPase domain (Fig. 2d). Surprisingly, the Trp90Phe mutation specifically abolished the interaction between rHsp70 and BMP while retaining the structural (folding as analysed by far- and near-ultraviolet circular dichroism) and functional (luciferase folding and ATP hydrolysis) aspects of the Hsp70 chaperone (Fig. 2d and data not shown). Thus, the rHsp70(Trp90Phe) mutant provided us with an invaluable tool to test further whether the direct interaction between Hsp70 and BMP endows Hsp70 with its lysosome protective attributes. Indeed, the rHsp70(Trp90Phe) mutant had completely lost its ability to protect the lysosomal membranes against photo-oxidation-induced destabilization, whereas the rHsp70(Trp580Phe) mutant showed the same protective effect as the wild-type protein (Fig. 2e). Notably, mutant Hsp70 proteins were endocytosed essentially as effectively as the wild-type Hsp70 (data not shown). Thus, we conclude that the binding of Hsp70 to BMP is essential for the lysosome-stabilizing effect of Hsp70.

Because the BMP concentration increases in endocytic vesicles as the endosomes mature to lysosomes<sup>14</sup>, pH-regulation might be the way by which Hsp70 is targeted to lysosomes. The theoretical isoelectric point (pI) of the ATPase domain of Hsp70 is 1.72 units higher than the peptide-binding domain (6.62 versus 4.9; as calculated using PROTPARAM, EXPASY proteomics server, Swiss Institute of Bioinformatics). This characteristic suggests that at acidic pH, the ATPase domain is preferentially positively charged, which could facilitate its interaction with anionic lipids. Our data demonstrating the dependence of Hsp70-BMP interaction on acidic pH and the ATPase domain support this theory. Furthermore, molecular modelling of the electrostatic surface of the ATPase domain of Hsp70 showed that it forms an almost wedge-like structure with a predominantly positive charge at the bottom of the wedge containing Trp 90, possibly explaining the profound effect of the Trp90Phe mutation on the ability of Hsp70 to interact with BMP and stabilize lysosomes (Fig. 2f).

Prompted by the fact that BMP binds ASM with high affinity and stimulates its ability to hydrolyse sphingomyelin<sup>13,14</sup>, we next asked whether Hsp70 could modulate ASM activity. The BIAcore analysis showed that pre-treatment of the BMP-containing LUVs with rHsp70 at sub-equimolar concentrations significantly facilitated the subsequent binding of recombinant ASM (rASM), whereas excess rHsp70 had an inhibitory effect (Fig. 3a). Remarkably, Hsp70 transgenic murine embryonic fibroblasts (Hsp70-MEFs), which are protected against stress-induced lysosomal damage<sup>1</sup>, showed significantly higher ASM activity than wild-type MEFs, as evidenced by an *in vitro* enzyme activity assay and quantitative analysis of total cellular ceramides (Fig. 3b, c and Supplementary Fig. 2). Furthermore, the treatment of wild-type MEFs with rHsp70 at a lysosome-stabilizing concentration (300 nM) significantly increased the ASM activity to a comparable level to that in Hsp70-MEFs (Fig. 3b). To test whether the Hsp70-associated activation of ASM could be responsible for the lysosome-stabilizing effect of Hsp70, we treated the cells with desipramine, a pharmacological ASM inhibitor<sup>18</sup>. Notably, desipramine reverted the lysosomal stress resistance of Hsp70-MEFs to the level of wild-type MEFs, as evidenced by accelerated loss of lysosomal membrane integrity after photo-oxidation (Fig. 3d). The lysosome-protective role of ASM was confirmed by the finding that lysosomes in U-2-OS cells depleted for ASM by three non-overlapping siRNAs, as well as in fibroblasts from a patient with NPD A (83/24), showed extreme sensitivity to photo-oxidation-induced damage (Fig. 3e, f, Supplementary Fig. 3 and Supplementary Movie 2). Notably, rHsp70 was also capable of enhancing the enzymatic activity of the endogenous mutated ASM as well as rASM delivered to the lysosomes by the endocytic pathway in NPD patient cells (Fig. 4a). It should be noted that akin to rHsp70, rASM also co-localized with the lysosomes (Supplementary Fig. 4). The increased ASM activity obtained by loading the lysosomes with rHsp70, rASM or the combination of the two proteins correlated with their ability to stabilize the

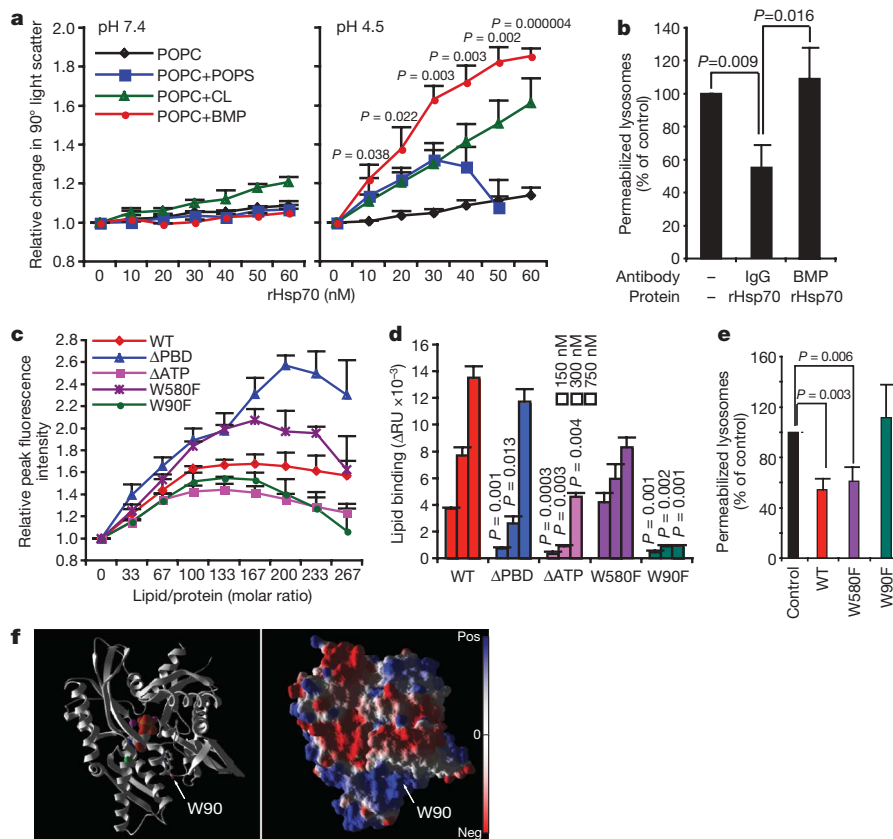


**Figure 2 | A pH-dependent interaction between Hsp70 and BMP stabilizes lysosomal membranes.** **a**, Relative changes in liposome 90° light scattering after addition of rHsp70 (in 0.02 nmol aliquots) to liposomes containing the indicated anionic lipids (each at  $\chi = 0.2$ ) at pH 7.4 (left) and pH 4.5 (right). CL, cardiolipin. **b**, U-2-OS cells were left untreated (–) or incubated with 50  $\mu\text{g ml}^{-1}$  anti-BMP or control IgG for 7 h before the addition of vehicle (–) or 300 nM rHsp70 for 24 h, and analysed for lysosomal integrity after photo-oxidation. **c**, Interaction of rHsp70 and its deletion ( $\Delta\text{ATP}$  and  $\Delta\text{PBD}$ ) and point (Trp90Phe (W90F) and Trp580Phe (W580F)) mutants with POPC and BMP ( $\chi = 0.2$ ) liposomes at pH 4.5, as measured by changes in relative peak fluorescence intensity. Protein concentrations were 30 nM and liposomes were added to yield 1  $\mu\text{M}$  concentration increments. **d**, BIAcore analysis of interactions of wild-type (WT) or mutant rHsp70 with immobilized LUVs at pH 4.5 (average diameter: 100 nm; total lipid concentration: 0.1 mM; composition: sphingomyelin ( $\chi = 0.1$ ), phosphatidylcholine ( $\chi = 0.5$ ), cholesterol ( $\chi = 0.2$ ) and BMP ( $\chi = 0.2$ )).

Liposomes were injected until equilibrium (100 s), and 150, 300 or 750 nM recombinant proteins in sodium acetate buffer (50 mM, pH 4.5) were injected for 200 s at a flow rate of 20  $\mu\text{l min}^{-1}$  followed by a dissociation phase for 10 min.  $\Delta\text{RU}$  is the difference between the response signal measured after liposome equilibrium and protein–liposome equilibrium. **e**, U-2-OS cells were left untreated (control) or incubated with indicated recombinant Hsp70 proteins (300 nM) for 24 h, and analysed for lysosomal integrity after photo-oxidation. **f**, Ribbon and molecular surface models of the ATPase domain of Hsp70. ATP (van der Waals-surface representation) can be visualized bound in the ATP-binding pocket. Green and purple spheres denote the van der Waals surface of the coordinated calcium and sodium ions, respectively. Notice the positively charged part of the domain in the bottom and the position of Trp 90. All values represent means  $\pm$  s.d. for a minimum of three independent experiments. *P* values are as compared with POPC liposomes (**a**) or the same concentration of wild-type Hsp70 (**d**), or as indicated (**b** and **e**).

lysosomes and to normalize the volume of the markedly enlarged lysosomal compartment in patient fibroblasts (Fig. 4a–c). Notably, the rHsp70(Trp90Phe) mutant that was unable to bind to BMP *in vitro* (Fig. 2d) also failed to normalize the lysosomes in NPD A cells (Fig. 4c). The ability of rHsp70 to revert the lysosomal pathology was not limited to a single ASM mutation, but it significantly decreased the volume of the lysosomal compartment and the sphingomyelin levels also in NPD A cells from another patient (no. 2), as well as in NPD B fibroblast lines carrying different mutations (Fig. 4c, d and Supplementary Fig. 5).

Taken together, our data indicate that the Hsp70–BMP interaction stabilizes lysosomes by a mechanism involving the regulation of sphingomyelin metabolism rather than direct physical stabilization of the membrane. Such an indirect effect is supported by the facts that a large part of the endolysosomal Hsp70 resides on the inner membranes<sup>1</sup>, and that BMP is exclusively localized to these membranes, where its major function is to support the disintegration and lipid extraction from lipid vesicles by ASM and sphingolipid activator proteins<sup>14</sup>. Interestingly, the ASM-mediated conversion of sphingomyelin to ceramide enhances membrane acyl chain order and increases lateral packing of lipids *in vitro*<sup>19</sup>. Furthermore, ASM-mediated increase in

lysosomal ceramide concentration modifies the steric conformation of lysosomal membranes in living cells and thereby facilitates their fusion with other intracellular vesicles and plasma membrane<sup>20,21</sup>. Thus, the changes in the lysosomal membrane composition and volume as a result of the ceramide-induced enhanced fusion capacity may contribute to the Hsp70-mediated increase in lysosomal stability. Conversely, various apoptotic stimuli induce the translocation of ASM to the outer leaflet of the plasma membrane, where ceramide can form lipid microdomains that function as sites for activation of membrane-associated signalling molecules involved in apoptotic signalling<sup>22</sup>. Thus, ceramide may have opposing effects on cell survival depending on whether it is produced inside the lysosome or in the plasma membrane.

The described molecular mechanism underlying the lysosome-stabilizing effect of Hsp70 may explain the recently reported surprising neuroprotective and behavioural effects of extracellular Hsp70 administered either to the sites of injury or intranasally<sup>23–25</sup>. Taken together with the reported neuronal effects of exogenous Hsp70 *in vivo*, our data greatly encourage the pre-clinical testing of the efficacy of exogenously administered rHsp70 alone or in combination with rASM in animal models of NPD.

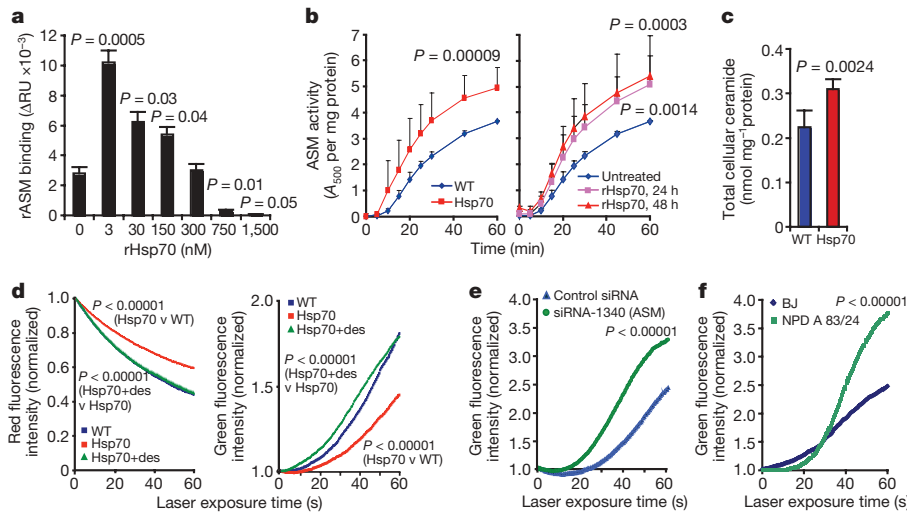


**Figure 3 | Hsp70 stimulates ASM activity that in turn stabilizes lysosomes.** **a**, BIAcore measurement of binding of 200 nM rASM to BMP-containing liposomes at pH 4.5 as a function of pre-bound rHsp70 ( $\Delta$ RU values for rHsp70 alone ranged from 48 to 18,441 at concentrations from 3 to 1,500 nM, respectively). The experiments were performed as in Fig. 2d, with rASM added for 180 s after the 10-min rHsp70-dissociation phase, followed by a 10-min dissociation phase for rASM. **b**, ASM activity in the lysates of wild-type and Hsp70 transgenic (Hsp70) MEFs (left), and in wild-type MEFs left untreated or treated with 300 nM rHsp70 for 24 or 48 h (right). **c**, Mass spectrometry analysis of total cellular ceramide (C16–C24) in wild-type and Hsp70 transgenic MEFs. For detailed analysis see Supplementary Fig. 2. **d**, Live single-cell imaging of the loss of lysosomal integrity after laser treatment in wild-type and Hsp70 MEFs, as well as in Hsp70 MEFs pre-incubated for 3 h with 12.5  $\mu$ M desipramine (des). Loss of

lysosomal red (left) and increase in cytosolic/nuclear green (right) fluorescence was continuously measured to give full kinetic curves for the loss of lysosomal integrity. A minimum of 25 cells from pre-defined areas were examined for each experiment. Note that wild-type and Hsp70+desipramine curves are nearly overlapping in the left panel. **e**, U-2-OS cells were transfected with control siRNA or RT-PCR-validated ASM siRNA (*SMPD1* siRNA-1340; Supplementary Fig. 3a), and 72 h later the loss of lysosomal integrity was analysed as in **d**. Similar results were obtained with two non-overlapping siRNAs (Supplementary Fig. 3). **f**, Lysosomal stability of fibroblasts from a healthy individual (BJ) and a patient with NPD A (83/24) were analysed as in **d**. All values represent means  $\pm$  s.d. for a minimum of three independent experiments. *P* values are as compared with no rHsp70 (**a**), wild-type cells (**b**, left and **c**), untreated cells (**b**, right), control siRNA (**e**, left), BJ cells (**e**, right), or as indicated (**d**).

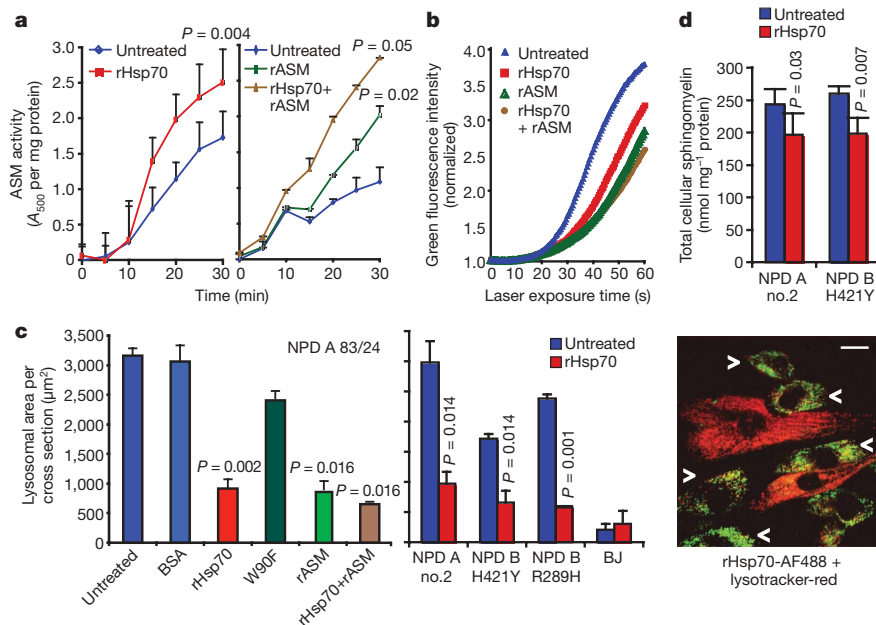


**Figure 4 | rHsp70 stimulates ASM activity, stabilizes lysosomes and reverts the lysosomal pathology in NPD fibroblasts.** **a**, ASM activity of NPD A (83/24) fibroblasts left untreated or treated with 300 nM rHsp70 for 48 h (left), or with 150 nM rASM alone or in combination with 300 nM rHsp70 for 24 h (right). *P* values were calculated from the obtained enzymatic velocity ( $\Delta A_{500 \text{ nm}}$  per mg protein per min). **b**, Lysosomal stability of NPD A (83/24) fibroblasts left untreated or treated for 24 h with 300 nM rHsp70, 150 nM rASM or a combination of rHsp70 and rASM was analysed as in Fig. 3d. *P* < 0.0001 for all treatments as compared with untreated cells. **c**, Quantification of lysosomal area of confocal cross sections of cells in NPD A (83/24) cells (left) and in indicated NPD and control (BJ) fibroblasts (right), left untreated or treated for 24 h with 300 nM BSA (negative control),

rHsp70 or rHsp70(Trp90Phe), 150 nM rASM, or a combination of 300 nM rHsp70 and 150 nM rASM. The residual ASM activities in the NPD fibroblasts used are shown in Supplementary Fig. 6. The picture on the right visualizes the effect of 24 h rHsp70 treatment (green) on the volume of the lysosomal compartment (red) in NPD A 83/24 fibroblasts. White arrowheads indicate cells with endocytosed rHsp70 and markedly decreased volume of the lysosomal compartment. Scale bar, 20  $\mu$ m. **d**, Mass spectrometry analysis of total cellular sphingomyelin (C16–C24) in indicated NPD fibroblasts left untreated or treated with 300 nM for 48 h. For detailed analysis see Supplementary Fig. 5. All the values represent means  $\pm$  s.d. for a minimum of three independent experiments. *P* values are as compared with untreated cells.

## METHODS SUMMARY

NPD A fibroblasts originate from a 5-month-old patient with hepatosplenomegaly (83/24) and an unknown source (no. 2). NPD B fibroblasts with homoallelic His412Tyr and Arg289His mutations are of Arabic and unknown parentages, respectively. The residual ASM activities in NPD fibroblasts are presented in Supplementary Fig. 6. Hsp70 transgenic and appropriate control MEFs were generated as described previously<sup>1</sup>. Recombinant proteins were generated using the pET-16b vector system and Ni<sup>2+</sup>-affinity-purification (Novagen), and labelled with Alexa Fluor 488 according to manufacturers protocol (Molecular Probes). To analyse the lysosomal integrity, we developed a real time imaging method of cells stained with acridine orange, a metachromatic weak base that accumulates in the acidic compartment of the cells staining them red and sensitizing them to photo-oxidation<sup>1,26</sup>. The photo-oxidation-induced loss of the lysosomal pH-gradient and leakage of acridine orange to the cytosol from individual lysosomes was quantified visually as a 'loss of red dots' or as a decrease in red and increase in green fluorescence by Zeiss LSM DUO Software in fibroblasts (see Supplementary Movies 1 and 2). The tryptophan fluorescence spectra and liposome 90° light scattering were measured in 20 mM HEPES or MES, 0.1 mM EDTA, pH 7.4 or 4.5, essentially as described previously<sup>27,28</sup>. Surface plasmon resonance measurements were performed with immobilized LUVs using a BIAcore 2000 system as described<sup>18</sup>. siRNAs were transfected with Oligofectamine (Invitrogen). Immunodetection was performed with standard protocols. ASM activity was analysed using an Amplex Red Sphingomyelinase Assay Kit from Molecular Probes, with modifications described previously<sup>20</sup>. Lipid analysis was performed using an Esquire ion-trap electrospray mass spectrometer from Bruker/Hewlett-Packard, and the data were analysed using Bruker DataAnalysis for LC/MSD Trap version 5.2. Statistical analysis was performed using a two-tailed, paired Student's *t*-test, and all groups of data were tested for the comparability of their variances using an F-test.

**Full Methods** and any associated references are available in the online version of the paper at [www.nature.com/nature](http://www.nature.com/nature).

**Received 4 March; accepted 24 November 2009.**

- Nylandsted, J. *et al.* Heat shock protein 70 promotes cell survival by inhibiting lysosomal membrane permeabilization. *J. Exp. Med.* **200**, 425–435 (2004).
- Hwang, J. H. *et al.* Spontaneous activation of pancreas trypsinogen in heat shock protein 70.1 knock-out mice. *Pancreas* **31**, 332–336 (2005).
- Gyrd-Hansen, M. *et al.* Apoptosome-independent activation of lysosomal cell death pathway by caspase-9. *Mol. Cell. Biol.* **26**, 7880–7891 (2006).
- Bivik, C., Rosdahl, I. & Ollinger, K. Hsp70 protects against UVB induced apoptosis by preventing release of cathepsins and cytochrome c in human melanocytes. *Carcinogenesis* **28**, 537–544 (2007).
- Doulias, P. T. *et al.* Involvement of heat shock protein-70 in the mechanism of hydrogen peroxide-induced DNA damage: the role of lysosomes and iron. *Free Radic. Biol. Med.* **42**, 567–577 (2007).
- Brunk, U. T., Neuzil, J. & Eaton, J. W. Lysosomal involvement in apoptosis. *Redox Rep.* **6**, 91–97 (2001).
- Leist, M. & Jäättelä, M. Four deaths and a funeral: from caspases to alternative mechanisms. *Nature Rev. Mol. Cell Biol.* **2**, 589–598 (2001).
- Guicciardi, M. E., Leist, M. & Gores, G. J. Lysosomes in cell death. *Oncogene* **23**, 2881–2890 (2004).
- Stoka, V., Turk, V. & Turk, B. Lysosomal cysteine cathepsins: signaling pathways in apoptosis. *Biol. Chem.* **388**, 555–560 (2007).
- Kirkegaard, T. & Jäättelä, M. Lysosomal involvement in cell death and cancer. *Biochim. Biophys. Acta* **1793**, 746–754 (2009).
- Mambula, S. S. & Calderwood, S. K. Heat shock protein 70 is secreted from tumor cells by a nonclassical pathway involving lysosomal endosomes. *J. Immunol.* **177**, 7849–7857 (2006).
- Quintern, L. E. *et al.* Acid sphingomyelinase from human urine: purification and characterization. *Biochim. Biophys. Acta* **922**, 323–336 (1987).
- Linke, T. *et al.* Stimulation of acid sphingomyelinase activity by lysosomal lipids and sphingolipid activator proteins. *Biol. Chem.* **382**, 283–290 (2001).
- Kolter, T. & Sandhoff, K. Principles of lysosomal membrane digestion: stimulation of sphingolipid degradation by sphingolipid activator proteins and anionic lysosomal lipids. *Annu. Rev. Cell Dev. Biol.* **21**, 81–103 (2005).
- Ferlinz, K., Hurwitz, R. & Sandhoff, K. Molecular basis of acid sphingomyelinase deficiency in a patient with Niemann-Pick disease type A. *Biochem. Biophys. Res. Commun.* **179**, 1187–1191 (1991).
- Daugaard, M., Rohde, M. & Jäättelä, M. The heat shock protein 70 family: highly homologous proteins with overlapping and distinct functions. *FEBS Lett.* **581**, 3702–3710 (2007).
- Kobayashi, T. *et al.* A lipid associated with the antiphospholipid syndrome regulates endosome structure and function. *Nature* **392**, 193–197 (1998).
- Kölzer, M., Werth, N. & Sandhoff, K. Interactions of acid sphingomyelinase and lipid bilayers in the presence of the tricyclic antidepressant desipramine. *FEBS Lett.* **559**, 96–98 (2004).
- Holopainen, J. M., Subramanian, M. & Kinnunen, P. K. Sphingomyelinase induces lipid microdomain formation in a fluid phosphatidylcholine/sphingomyelin membrane. *Biochemistry* **37**, 17562–17570 (1998).
- Goñi, F. M. & Alonso, A. Sphingomyelinases: enzymology and membrane activity. *FEBS Lett.* **531**, 38–46 (2002).
- Utermöhlen, O., Herz, J., Schramm, M. & Kronke, M. Fusogenicity of membranes: the impact of acid sphingomyelinase on innate immune responses. *Immunobiology* **213**, 307–314 (2008).
- Smith, E. L. & Schuchman, E. H. The unexpected role of acid sphingomyelinase in cell death and the pathophysiology of common diseases. *FASEB J.* **22**, 3419–3431 (2008).
- Tidwell, J. L., Houenou, L. J. & Tytell, M. Administration of Hsp70 *in vivo* inhibits motor and sensory neuron degeneration. *Cell Stress Chaperones* **9**, 88–98 (2004).
- Yu, Q., Kent, C. R. & Tytell, M. Retinal uptake of intravitreally injected Hsc/Hsp70 and its effect on susceptibility to light damage. *Mol. Vis.* **7**, 48–56 (2001).
- Flerov, M. A. *et al.* The use of HSP70 for prevention of consequences of unavoidable stress in rats. *Bull. Exp. Biol. Med.* **136**, 120–122 (2003).
- Brunk, U. T., Dalen, H., Roberg, K. & Hellquist, H. B. Photo-oxidative disruption of lysosomal membranes causes apoptosis of cultured human fibroblasts. *Free Radic. Biol. Med.* **23**, 616–626 (1997).
- Holopainen, J. M., Saily, M., Caldentey, J. & Kinnunen, P. K. The assembly factor P17 from bacteriophage PRD1 interacts with positively charged lipid membranes. *Eur. J. Biochem.* **267**, 6231–6238 (2000).
- Zhao, H. & Kinnunen, P. K. Binding of the antimicrobial peptide temporin L to liposomes assessed by Trp fluorescence. *J. Biol. Chem.* **277**, 25170–25177 (2002).

**Supplementary Information** is linked to the online version of the paper at [www.nature.com/nature](http://www.nature.com/nature).

**Acknowledgements** We thank E. Gulbins and A. Riehle for the NPD A (no. 2) cells, the Charité Berlin and the Johannes Gutenberg-Universität Mainz for the NPD B fibroblasts, C. Ejising and H. Schulze for advice, and J. Grünberg, B. Margulis and the Developmental Studies Hybridoma Bank for antibodies. This work was supported by grants from the Danish Cancer Society, the Danish National Research Foundation, the Danish Medical Research Council, the European Commission FP7 (APO-SYS), the Meyer Foundation, the Novo Nordisk Foundation, and the Association for International Cancer Research for M.J., the Finnish Academy and the Sigrid Juselius Foundation for P.K.J.K., Volkswagenstiftung for A.G.R. and C.A., Deutsche Forschungsgemeinschaft (SFB 645, SPP 1267) and EU (LipidomicNet) for K.S., and the Polish Ministry of Science and High Education for A.Z.

**Author Contributions** T.K. and M.J. designed the study, analysed the data and wrote the paper. T.K. performed experiments for Figs 1a–e, 2b, e, f, 3b, d, f, 4a–c, Supplementary Figs 1, 4 and Supplementary Movies. A.G.R. and C.A. performed experiments for Figs 2d, 3a and Supplementary Fig. 6, and provided NPD cell lines. K.S. contributed to the BIAcore data and provided rASM. N.H.T.P. performed experiments for Fig. 3e and Supplementary Fig. 3. P.K.J.K. designed the biophysical studies on Hsp-lipid interactions. A.K.M. and I.M. performed experiments for Fig. 2a, e. O.D.O. and J.K. performed experiments for Figs 3c, 4d and Supplementary Figs 2 and 5. A.Z. validated the functionality of rHsp70 and its mutants, and provided proteins for control. J.N. provided input to study design. All authors discussed the results and commented on the manuscript.

**Author Information** Reprints and permissions information is available at [www.nature.com/reprints](http://www.nature.com/reprints). The authors declare no competing financial interests. Correspondence and requests for materials should be addressed to M.J. ([mj@caner.dk](mailto:mj@caner.dk)).

## METHODS

**Assays for lysosomal integrity.** Sub-confluent cells incubated with  $2 \mu\text{g ml}^{-1}$  acridine orange for 15 min at  $37^\circ\text{C}$  were washed, irradiated and analysed in Hank's balanced salt solution complemented with 3% FCS. Cells from eight pre-defined areas were visualized and exposed to blue light from USH102 100W mercury arc burner (Ushio electric) installed in a U-ULS100HG housing (Olympus) for 20 s. Fluorescence microscopy was performed on Olympus IX-70 inverted microscope with a LCPlanFl  $\times 20$  objective with numerical aperture (NA) = 0.40. Loss of lysosomal pH gradient was quantified by counting the loss of intense red staining. A more elaborate method was developed to handle the larger lysosomal compartment of the various fibroblasts. Cells were exposed to 489 nm light from a 100-mW diode laser while laser scanning micrographs were captured every 330 ms on a Zeiss LSM LIVE DUO confocal system in two channels defined by bandpass filters for 495–555 nm (green) and LP650 nm (red) light. Cells in the pre-defined areas were subsequently analysed by the integrated Zeiss LSM DUO software.

**Immunodetection and microscopy.** Primary antibodies used included mouse monoclonal antibodies against Hsp70 (2H9; kindly provided by B. Margulis, Russian Academy of Sciences), glyceraldehyde-3-phosphate dehydrogenase (GAPDH; Biogenesis), BMP (6C4)<sup>17</sup> and LIMP-1 (H5C6; the Developmental Studies Hybridoma Bank, University of Iowa). Proteins were separated by 10% SDS-PAGE, transferred to a nitrocellulose membrane, and were detected with indicated primary antibodies, peroxidase-conjugated secondary antibodies from Dako, ECL western blotting reagents (Amersham), and Luminescent Image Reader (LAS-1000Plus, Fujifilm). For immunocytochemistry, Alexa-Fluor-576- or Alexa-Fluor-488-conjugated secondary antibodies were used. LysoTracker-Red was used for live visualization of the lysosomal compartment. Fluorescence images were taken using a Zeiss Axiovert 100M laser scanning microscope. LysoTracker quantification and timelapse movies for lysosomal integrity were done on a Zeiss LSM LIVE DUO system. Co-localization was validated by calculating Pearson's and Mander's coefficients.

**Tryptophan fluorescence spectra and liposome  $90^\circ$  light scattering.** The tryptophan fluorescence spectra (RFI) and liposome  $90^\circ$  light scattering (RSI) were analysed in 20 mM HEPES or MES, 0.1 mM EDTA, and pH 7.4 or 4.5 using LUVs consisting of the indicated lipids essentially as described previously<sup>27,28</sup>. For the RFI, LUVs were added in 10- $\mu\text{M}$  aliquots and spectra recorded after a 20-min stabilization period. For RFI, pegylated cuvettes were used to reduce binding of protein to glass, LUVs were added in aliquots yielding an increase by 1  $\mu\text{M}$  in concentration, and spectra were recorded after a 20-min stabilization period. For the RSI, recombinant proteins were added in 0.02-nmol aliquots.

**Surface plasmon resonance (BIAcore).** For preparation of LUVs, a lipid mixture consisting of 10mol% sphingomyelin, 50mol% phosphatidylcholine, 20mol% cholesterol and 20mol% BMP dissolved in organic solvents, was dried under a stream of argon and rehydrated in Tris-HCl buffer (pH 7.4)<sup>18</sup>. The mixture was freeze-thawed nine times in liquid nitrogen and then in an incubator at  $37^\circ\text{C}$ . After ultrasound bath for 15 min, the mixture was passed 21 times through a polycarbonate membrane with a pore diameter of 100 nm. Surface plasmon resonance measurements were performed using a BIAcore 2000 system at  $25^\circ\text{C}$ . LUVs (total lipid concentration 0.1 mM) were immobilized on the surface of an L1 sensor chip (BIAcore) in PBS (loading buffer). The running buffer used was sodium acetate buffer (50 mM, pH 4.5). As a control, ASM (0.2  $\mu\text{M}$ , 60  $\mu\text{l}$  in running buffer) was injected directly on the liposome surface.

Response units between 4,100 and 5,250 were obtained. The protein of interest was injected in running buffer at a flow rate of  $20 \mu\text{l min}^{-1}$  at the concentrations indicated. After injection, a dissociation phase of 10 min was appended. In the case where rASM followed rHsp70, rASM was added for 180 s after the 10 min rHsp70-dissociation phase followed by a 10-min dissociation phase.

**RNA interference.** siRNAs were designed against sequences in *HSPA1A* and *HSPA1B* (5'-GGCCATGACGAAAGACAACAATCTGT-3') or *ASM* (*SMPD1*; 1340: 5'-GAGGATCGAGGAGACAAAGTGCATA-3'; 938: 5'-CCCGCACATGATGTCTGGCACCAGA-3'; 1257: 5'-CCCGTGAGAACTTCTGGCTCTTGAT-3'). The control siRNA (5'-CGACCGAGACAAGCGCAAG-3') has been described previously<sup>29</sup>. All siRNAs were purchased from Invitrogen.

**Lipid analysis.** The lipids from cells collected in ice-cold PBS were extracted using the Bligh and Dyer<sup>30</sup> method exchanging water with 0.88% KCl. Internal standards (0.5 nmol PHS C18 ceramide from Avanti Polar Lipids and 5 nmol C17 sphingomyelin from S. Sonnino) were added in the beginning of the extraction. The chloroform phase was dried under a stream of nitrogen, dissolved in 25  $\mu\text{l}$  chloroform/methanol (3:1, v/v) and the lipids were separated on a YMC, PVA-SIL (PV12S051501QT)  $150 \times 1.0 \text{ mm i.d. S-5}\mu\text{m}$ ,  $120 \text{ \AA}$  column. The solvents were A: hexane (98%)/isopropanol (2%), 0.1% TEA equimolar formic acid, B: MTBE/isopropanol (45/55, v/v), 0.1% TEA equimolar formic acid, and C: methanol 0.1% TEA and 2 $\times$  molar excess formic acid. The column was equilibrated with 12% A and 88% B. Lipids were eluted with a flow of  $45 \mu\text{l min}^{-1}$  using a laminar gradient as follows: at 3 min 9.8% A, 74.2% B and 16% C, at 4 min 7.6% A, 64.1% B and 31% C, at 5 min 100% C, at 11 min 100% C, at 13 min 100% B, at 17 min 12% A and 88% B, at 24 min 12% A and 88% B. The analysis was performed using an Esquire ion trap electrospray mass spectrometer from Bruker/Hewlett-Packard, and data were analysed using Bruker DataAnalysis for LC/MSD Trap version 5.2. Nitrogen was used as the drying gas ( $7.5 \text{ l min}^{-1}$  at  $260^\circ\text{C}$ ). In the negative-ion mode (ceramide analysis), the potentials of the spray needle, capillary exit and skimmers 1 and 2 were  $-4,000$ ,  $-127.3$ ,  $-60$  and  $-5 \text{ V}$ , respectively. In the positive-ion mode (sphingomyelin analysis), the respective potentials were  $+4,000$ ,  $+127.3$ ,  $+60$  and  $+5 \text{ V}$ .

**Molecular modelling.** Molecular modelling of human Hsp70 was done with software available from the Expert Protein Analysis System (EXPaSy) proteomics server of the Swiss Institute of Bioinformatics (<http://expasy.org/>) and DeepView-Swiss PDB Viewer<sup>31</sup> on the basis of the crystal structures of the ATPase (Protein Data Bank (PDB) accession: 1S3X)<sup>32</sup> and the peptide-binding (PDB accession 7HSC)<sup>33</sup> domains. Surface models were on the basis of coulomb interaction at pH 7.0, using a solvent dielectric constant of 80 ( $\text{H}_2\text{O}$ ).

- Rohde, M. *et al.* Members of the heat-shock protein 70 family promote cancer cell growth by distinct mechanisms. *Genes Dev.* **19**, 570–582 (2005).
- Bligh, E. G. & Dyer, W. J. A rapid method of total lipid extraction and purification. *Can. J. Biochem. Physiol.*, **37**, 911–917 (1959).
- Guex, N. & Peitsch, M. C. SWISS-MODEL and the Swiss-PdbViewer: an environment for comparative protein modeling. *Electrophoresis* **18**, 2714–2723 (1997).
- Sriram, M., Osipiuk, J., Freeman, B., Morimoto, R. & Joachimiak, A. Human Hsp70 molecular chaperone binds two calcium ions within the ATPase domain. *Structure* **5**, 403–414 (1997).
- Morshausen, R. C. *et al.* High-resolution solution structure of the 18 kDa substrate-binding domain of the mammalian chaperone protein Hsc70. *J. Mol. Biol.* **289**, 1387–1403 (1999).